



## Multi-objective Optimal Design of Driving Spring in Slide Cover Hinge

Alan C. Lin<sup>1</sup> and Tu-Chuan Wang<sup>2</sup>

<sup>1</sup> National Taiwan University of Science and Technology, [alin@mail.ntust.edu.tw](mailto:alin@mail.ntust.edu.tw)

<sup>2</sup> National Taiwan University of Science and Technology, [wangtc@mail.sju.edu.tw](mailto:wangtc@mail.sju.edu.tw)

### ABSTRACT

Combining Taguchi experimental design and fuzzy theory, this research aims to develop a multi-objective algorithm to determine the optimal design parameters for the driving springs in a slide cover hinge. The goal is to determine parameters that will meet the two basic requirements of the spring that would generate adequate reaction force but minimize maximum stress. This research applies finite element method to calculate the reaction force and maximum stress of a deformed spring. Meanwhile, the Taguchi method, which could dramatically reduce the number of experiments, is used to determine the optimal design parameters for the spring. Experimental results suggest that if the maximum stress is minimized, the reaction force will decrease, resulting in the autonomous release of the slide cover hinge; if adequate reaction force is achieved, the maximum stress would exceed the design standard. Therefore, this research employs fuzzy theory to achieve multi-objective as “minimization of maximum stress” and “sufficient reaction force”, as a result of an optimal design for driving springs in a slide cover hinge.

**Keywords:** finite element method, Taguchi method, Fuzzy theory, multi-objective algorithm, slide cover hinge.

**DOI:** 10.3722/cadaps.2013.827-838

### 1 INTRODUCTION

Due to the popularity of cell phones, the communications industry has developed considerably, and trend towards a more innovative design, not only including more accessible functions, but also being user-friendly. Currently, sliding cell phones are well accepted by the market due to its compact size and is effective against unintentional button-pushes. Fig. 1 shows a physical example of slide cover hinge. When a user pushes the slider, the spring generates a reaction force along the pushing direction. In this case, an inappropriately designed spring would be problematic, for example, an over stress will lead to shorter product life, or an insufficient reaction force will result in a loose sliding mechanism.

The driving spring in a slide cover hinge is normally not standardized. Hence, it is unlikely to employ the equations from the mechanical design handbook to calculate its associated stress or reaction force. Also, it is infeasible to manufacture the spring and to decide the optimal specifics experimentally, because it is a time-consuming and costly procedure. Fortunately, the development of

current computer technologies allows more options for design and product analysis. During the design stage, not only both shape and dimension of the spring is defined, its associated stress, elastic deformation and reaction force are also analysed by these design tools, where finite element method is one of the most important analysis approach. In this paper, finite element method is utilized to define design parameters and boundary conditions to analyse the deformed spring, its required force as well as the internal stress distribution. Then an optimal design is obtained to improve the plastic deformation or other destructive problem due to over stress caused by elastic movement of the spring, thus extending the product life of the driving spring.

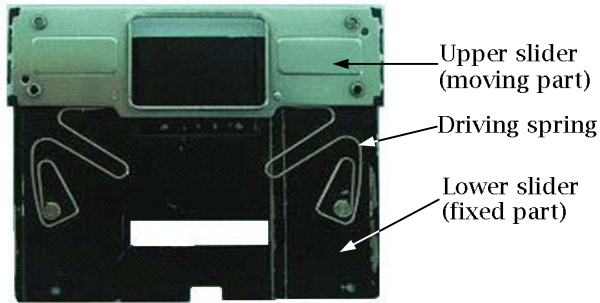


Fig. 1: Sample of slide cover hinge.

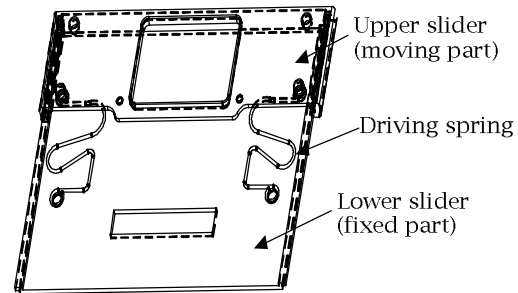


Fig. 2: 3D CAD model of slide cover hinge.

In literature, the finite element method (FEM) has been widely used in solving various types of engineering problems, for instance, structural analysis, heat transfer, fluid mechanics, and electromagnetism [1~3]. This paper focuses on applying FEM to conduct structural analyses for a continuously deforming spring. There are many case studies of structural analysis and improvement in conjunction with finite element analysis and optimal design. For instance, Ou and Balenrea [4] used FEM to simulate the forging of aerofoil sections to investigate the effect of variations in parting line and friction on material flow, forging force history, and elastic deflections. Hsu et al. [5] used ANSYS, a well-known CAE software, to optimize designs for electronic connectors, achieving an optimal insertion force. Another popular approach of design analysis is the Taguchi method. This method is based on statistical principles, and was developed to determine the optimum number of experiments to reduce experimental cost and maximize data reliability [6]. The general procedure of this approach is to apply an orthogonal array to decide experimental content, then to employ variation analysis and signal/noise ratio to determine and measure characteristics that may affect the final product. By applying the concept of design parameters, product variance will reduce and results in improved product robustness. Since the Taguchi method is a general method, this methodology is widely applicable in various fields. For example, Lin et al. [7] were able to determine the optimal combination of electrode-wear and material removal rate during electrical discharge machining. Kunjur and Krishnamurty et al. [8] developed a robust multi-criteria optimization approach, which is based on the Taguchi method, and integrated it with statistical variation analysis to estimate relative dominance and significance of design factors and to provide sufficient information for selecting levels of design parameters. Similarly, Tarng et al. [9] also combined the Taguchi method with fuzzy theory to develop a multi-criteria algorithm. This method allows users to integrate multiple characteristics into one, and to obtain the optimized result for all control factors. Similar research projects were also studied by several researchers [10~14]

Fig. 1 shows the sliding mechanism of a slide cover hinge. The system includes three major components: driving spring, moving part (upper slider) and fixed part (lower slider). Normally there is a 0.03mm gap between upper and lower sliders. The two ends of the driving spring are attached to the sliders separately. When moving the upper slider forwards or backwards, the spring deforms accordingly. Once the moving part travels beyond halfway, the spring releases its stored energy to push the slider into the desirable position, which is the basic sliding mechanism of the system. Since the slider-type cell phone is a modern 3C product, applying FEM to a slide spring has been rarely observed in previous research. In this work, a detailed description of employing FEM to analyze the non-linear stress during elastic deformation of the slide spring is presented. Furthermore, the use of

this analysis as a basic operation and the implementation of the Taguchi method is also included. In brief, this approach aims to obtain the optimal design parameters for the spring, and to minimize the stress generated during the deformation process to extend the life cycle of the spring.

## 2 REACTION FORCE AND STRESS ANALYSIS OF DRIVING SPRING

Fig. 2 illustrates the 3D CAD model of a slide cover hinge. Fig. 3 shows a flow chart describing how the finite element method is used to calculate the spring's reaction force and stress. Firstly, the type of mesh elements is selected. After homogenizing the material of the spring, the material is segmented into pieces of mesh elements, followed by defining the boundary conditions. Finally, the stress and forces are simulated and calculated. The step-by-step methods are explained below:

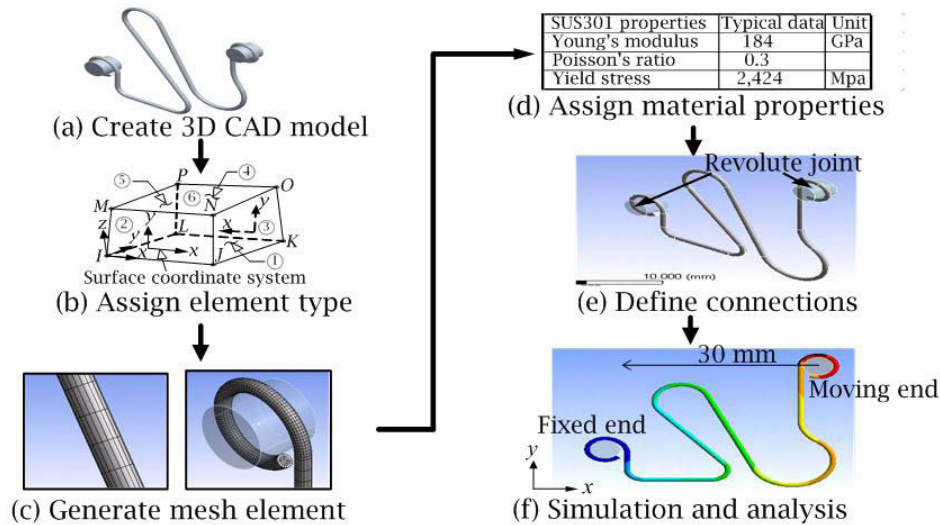


Fig. 3: Flow chart of finite element analysis for driving spring.

- **Creation of 3D CAD Model:** firstly a 3D CAD model was established for analyzing the driving spring. In this research, a 3D CAD model is built by Pro/Engineer, as shown in Fig. 3(a).
- **Selection of Element Type:** This research uses ANSYS Workbench to analyze the stress of the driving spring. When the user moves the slider, there is a significant elastic deformation of the spring itself, where a large deflection is used for the analysis. Taking both accuracy and efficiency of the calculation into consideration, a reduced integration is applied for the numeration. As the spring analysis is a structural-analysis process, and requires 6 degrees of freedom, thus, a hexahedron, which includes 8 vertices, is used for spring analysis.
- **Generating the Mesh Element:** After developing the 3D CAD model, it is necessary to convert it in a mesh grid for further finite element analysis. In this paper, the spring is made from a metal wire with circular cross-sections. The element size for the cross section is given as 0.065, as shown in Fig. 3(c). The mesh of the spring can be classified into 2 categories, circular-segment's mesh with size 0.1mm, and linear-segment's mesh with size 0.12mm due to the simplicity of stress distribution.
- **Assignment of material Properties:** the material of the driving spring is assumed as homogeneous and isotropic, and it is in agreement with von-Mises yield criterion. The material used in this research is annealed SUS301 with Young's modulus = 184GPa and Poisson's ratio = 0.3.
- **Defining Connections:** During the spring's elastic deformation, one end of the spring is driven by a moving rivet, while the other end is attached to a fixed rivet. The connection between the spring and rivet at both ends are assumed as revolute joint.
- **Simulation and Analysis:** As shown in Fig. 1, a sliding mechanism has two springs, each for one side. The spring is made from stainless steel wires with a diameter of 0.45mm. During elastic deformation, the spring should provide at least 150gf force as reaction. Since only one spring

is analyzed, the reaction for each spring should exceed 75gf. Meanwhile, the sliding distance is assumed as 30mm, and the distance between the center points of the moving and fixed rivets is 10.5mm. In addition, the static analysis, which is not time related, is applied for simulating the elastic deformation, stress and reaction, while the large deflection is used to determine the analysis mode, and the moving rivet supposes to slide 30mm along x direction. When the moving end of the spring travels against the x direction, the spring itself generates reaction forces, on which a finite element analysis is used to acknowledge how the stress and reaction varies through the procedure. Fig. 4 indicates the variation of von-Mises stress, where the horizontal axis is time, vertical axis is the stress, and the maximum stress was recorded at 0.53125s at 1752.4 MPa.

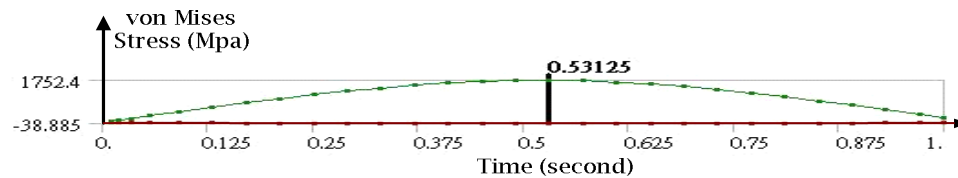


Fig. 4: von Mises stress graph.

### 3 OPTIMAL DESIGN PARAMETERS OF DRIVING SPRING

This research combines Taguchi method, multiple performance characteristics index (MPCI), and fuzzy theory to develop a multi-objective algorithm, in order to decrease the maximum stress and reach appropriate reaction force, consequently to achieve a better combination of design parameters. Taguchi method uses an orthogonal array to determine the number of necessary experiments. During the analysis stage, MPCI considers more than two characteristics indices, which increases the reliability of data analysis. Fuzzy theory permits the gradual assessment with the aid of membership function to describe attributes of an objective. Fig. 5 is a flow chart of optimal design for a driving spring. The details of each step are discussed below.

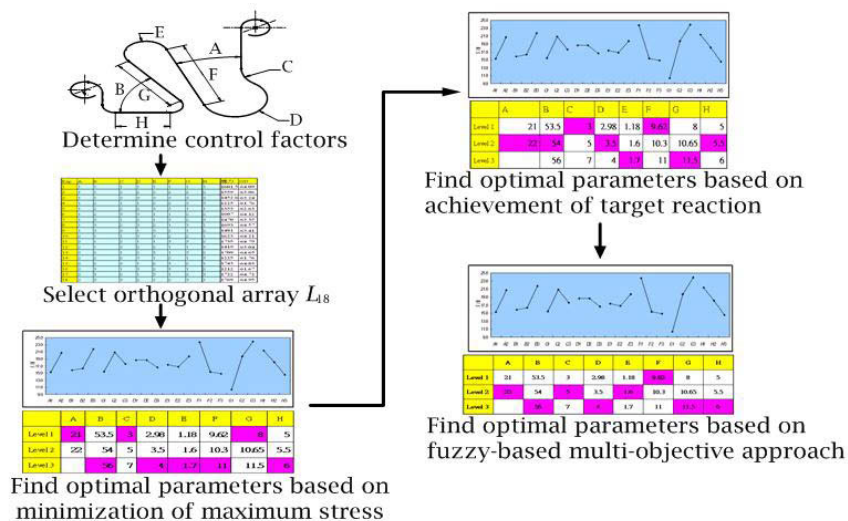


Fig. 5: Flow chart of optimal design of driving spring.

#### 3.1 Setting Control Factors and its Levels

Since this research investigates the stress and reaction force induced by spring movements, the stress and reaction force are targeted as the characteristics index for Taguchi methods. As shown in Fig. 5., the shape of the spring is mainly determined by 8 specific dimensions, which include 2 angles (A, B), 3 radii (C, D, E), and 3 lengths (F, G, H), while other dimensions remain constant. Due to the space limit for sliding, each dimension can only vary within a certain range. If a dimension is variable, this

dimension is known as a “control factor” in the Taguchi method. Furthermore, a comprehensive combination of the factors at all the levels would lead to an optimal design, however, this procedure requires a substantial number of experiments. Thus, the Taguchi design of experiment is employed to achieve the same optimal design, but with reduced experiment size. In the context of this research, the 8 abovementioned dimensions are selected for experiments to seek an optimal design for the spring, which could generate sufficient reaction force but minimize stress.

Then, it is necessary to define the variance of each factor, namely, the levels. At this stage, it is also important to confirm that there is no interference within the spring when the moving end slides towards x direction. Tab. 1 lists the levels of above 8 control factors.

Control Factor	Angle (degree)		Radius (mm)			Length (mm)		
	A	B	C	D	E	F	G	H
Level 1	21	53.5	3	2.98	1.18	9.62	8	5
Level 2	22	54	5	3.5	1.6	10.3	10.65	5.5
Level 3		56	7	4	1.7	11	11.5	6

Tab. 1: Summary of levels of 8 control factors.

### 3.2 Application of L18 Orthogonal Array for Taguchi Methods

As shown in Tab. 1., factor A contains 2 levels, while the rest have 3 levels. Thus, the  $L_{18}(2^1 \times 3^7)$  orthogonal array is used. According to this table, the finite element analysis of each level is preformed 18 times in total, then the maximum stress and reaction force along x axis can be obtained.

### 3.3 Implementing “Smaller-the-better of Maximum Stress” to Perform Taguchi Analysis

To enhance the durability of the spring, stress generated during the movement of sliders must be kept to a minimum. Thus, in this research, “smaller-the-better of maximum stress” is the primary characteristics when applying Taguchi analysis for an optimal design.

The Taguchi method uses S/N ratio as a value of measuring the performance characteristic, and the formula of S/N ratio calculation is shown below:

$$S/N = -10 \log_{10} \left( \frac{1}{n} \sum_{i=1}^n y_i^2 \right) \quad (1)$$

where S/N =quality characteristic of maximum stress,  $y_i$  =maximum stress at ith experiment, and  $n$  = number of experiments.

Exp.	Max stress (MPa)	S/N ratio	Exp.	Max stress (MPa)	S/N ratio
1	1601.5	-64.09	10	1623	-64.21
2	1559	-63.86	11	1735	-64.79
3	1452.6	-63.24	12	1419	-63.04
4	1225	-61.76	13	1709	-64.65
5	1353	-62.63	14	1225	-61.76
6	1607	-64.12	15	1743	-64.83
7	1470	-63.35	16	1212	-61.67
8	1693	-64.57	17	1722	-64.72
9	1481	-63.41	18	1769	-64.95

Tab. 2: Maximum stresses and associated S/N ratios of the driving spring.

This research applies finite element software to perform the analysis. And each group of experimental data in  $L_{18}(2^1 \times 3^7)$  orthogonal array is calculated once, thus,  $n = 1$ . According to the flow chart of finite element analysis in Fig. 3, the maximum stress of each experiment can be obtained. For instance, in experiment #1, the spring geometries are  $A=21^\circ$ ,  $B=53.5^\circ$ ,  $C=3$  mm,  $D=2.98$  mm,  $E=1.18$  mm,  $F=9.62$  mm,  $G=8$  mm,  $H=5$  mm (see Tab. 1.). After performing the finite element analysis, the maximum stress is calculated as 1,601.5Mpa. Tab. 2 lists the maximum stresses and the corresponding stress S/N ratios for the 18 experiments. From the table, the S/N ratio of 8 control factors at each level can be obtained.

Tab. 3 indicates the S/N ratio of stress of the 8 control factors at each level. And Fig. 6 is a response graph of those S/N ratios aiming to observe the relative inter-relationships.

Control Factor	A	B	C	D	E	F	G	H
Level 1	-63.45	-63.87	-63.29	-63.93	-63.84	-64.20	-62.77	-64.21
Level 2	-63.85	-63.29	-63.72	-63.75	-63.29	-63.33	-64.18	-63.75
Level 3		-63.78	-63.93	-63.26	-63.81	-63.42	-64.00	-62.98

Tab. 3: S/N ratios of maximum stress of 8 control factors at various levels.

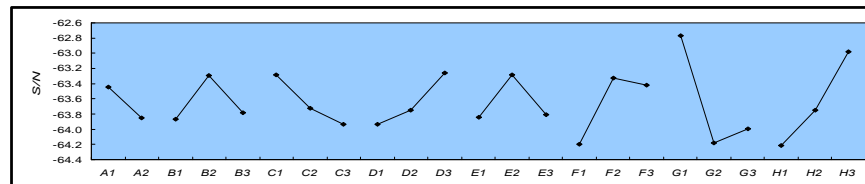


Fig. 6: Response graph of the S/N ratio of maximum stress.

According to the Taguchi theory, a higher S/N ratio represents a better characteristic. Hence, from Fig. 6, the optimal combination of spring dimensions is A1 B2 C1 D3 E2 F2 G1 H3. Then the finite element analysis is applied to calculate its maximum stress as 1,150.1MPa, and maximum reaction force as 0.3258N (33.21gf). Comparing with experimental results in Tab. 2, while maximum stress decreases significantly, the reaction force is too small to move the slider (as mentioned before, the sliding system requires at least 150gf). To avoid this problem, the next step is to implement a “fixed reaction force” as the optimal goal.

### 3.4 Implementing “Nominal-the-best of Reaction Force” to Perform Taguchi Analysis

After the experiments of the sliding system, a 70gf reaction force can provide a better handling of the sliders, and the value is targeted as the objective reaction force in this research. Thus the S/N ratio calculations are as follows:

$$S/N = -10 \log_{10}(y - m)^2 \quad (2)$$

Where  $S/N$  = quality characteristic of maximum stress,

$y$  = maximum reaction force, and

$m$  = target reaction force, 70gf (0.6867N).

From finite element analysis, the maximum reaction force of each experiment can be obtained, and the S/N ratio of reaction force can be calculated according to Eq. (2). Tab. 4 summarizes the maximum reaction forces and the corresponding S/N ratios for the 18 experiments.

<i>Exp.</i>	<i>Max. reaction (N)</i>	<i>S/N ratio</i>	<i>Exp.</i>	<i>Max. reaction (N)</i>	<i>S/N ratio</i>
1	0.52357	15.75	10	0.60206	21.45
2	0.57799	19.27	11	0.66554	33.49
3	0.53278	16.25	12	0.45738	12.79
4	0.35279	9.53	13	0.75901	22.82
5	0.40577	11.03	14	0.35279	9.53
6	0.5924	20.51	15	0.65804	30.85
7	0.4938	14.29	16	0.34715	9.38
8	0.71797	30.10	17	0.71394	31.30
9	0.4715	13.34	18	0.70502	34.74

Tab. 4: Maximum reaction forces and associated S/N ratios of the driving spring.

The results in Tab. 4 can be used to calculate the S/N ratio of reaction force of 8 control factors at each level. Tab. 5 lists the results of S/N ratios of reaction force for the 8 control factors at each level, which are plotted in a response graph as shown in Fig. 7.. From the figure, the optimal combination of spring dimensions is A2 B3 C2 D1 E1 F1 G3 H1. Then the finite element analysis is applied to calculate its maximum stress as 1,840.3MPa, and the maximum reaction force as 0.7014N (71.5gf). This reaction force is close to the target value, however, the high maximum stress may result in spring damage.

<i>Control Factor</i>	<i>A</i>	<i>B</i>	<i>C</i>	<i>D</i>	<i>E</i>	<i>F</i>	<i>G</i>	<i>H</i>
<i>Level 1</i>	16.68	19.83	15.54	22.38	21.39	22.21	11.97	23.99
<i>Level 2</i>	22.93	17.38	22.45	19.16	18.65	17.98	22.95	19.80
<i>Level 3</i>		22.19	21.42	17.87	19.36	19.22	24.49	15.61

Tab. 5: S/N ratios of maximum reaction force of 8 control factors at various levels.

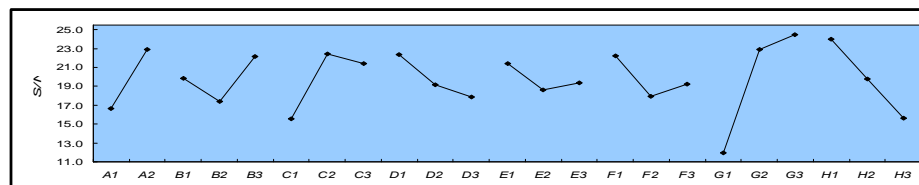


Fig. 7: Response graph of the S/N ratio of maximum reaction force.

### 3.5 Apply Fuzzy-based Taguchi Method to Find Multiple Performance Characteristics Index

The above experiments and analysis show that the application of Taguchi method is unable to simultaneously meet the two requirements - reduced stress and fixed reaction force. To solve the problem, a fuzzy-based Taguchi method is proposed. The fuzzy theory is firstly employed to combine more than two quality characteristics into one single characteristic, and then the Taguchi method is applied for stress analysis, which would attain the requirements of multiple performance characteristics index (MPCI). The two objectives set for spring design are to minimize the stress, and to provide target reaction force 75gf (note: as both characteristics are considered at the same time, the target value should be reduced slightly; hence, the objective reaction force was adjusted from 70gf to 75gf). According to Eq. (2), the S/N ratios of reaction force are calculated for each of the experiments. The results are summarized in Tab. 6.

<i>Exp.</i>	<i>Reaction force (N)</i>	<i>S/N ratio</i>	<i>Exp.</i>	<i>Reaction force (N)</i>	<i>S/N ratio</i>
1	0.52357	13.47	10	0.60206	17.48
2	0.57799	16.04	11	0.66554	23.07
3	0.53278	13.85	12	0.45738	11.11
4	0.35279	8.34	13	0.75901	32.67
5	0.40577	9.63	14	0.35279	8.34
6	0.59240	16.87	15	0.65804	22.19
7	0.49380	12.33	16	0.34715	8.21
8	0.71797	35.00	17	0.71394	33.23
9	0.47150	11.56	18	0.70502	30.25

Tab. 6: Summary of analysis results when target reaction force is 75gf.

Fig. 8 illustrates the fuzzy theory model proposed by Mamdani [15]. The left of the graph are the inputs, including the stress and reaction force, while the right is the output from the fuzzy model. In order to achieve the multiple objective, this approach applies triangle membership function to convert the S/N ratios of maximum stress and reaction force into a set of membership degrees in terms of S, M and L as the inputs for the fuzzy theory model. The output of this model also uses triangle membership function to group the results into 5 degrees as VS, S, M, L and VL, listed in Tab. 7. Details to implement the proposed fuzzy-based Taguchi method are discussed below.

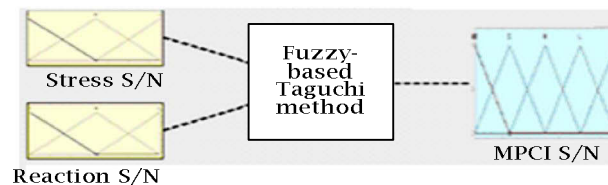


Fig. 8: S/N ratio in the fuzzy-based Taguchi method.

<i>Rule number</i>	<i>S/N of max. stress</i>		<i>and</i>	<i>S/N of target reaction</i>		<i>then</i>	<i>S/N of MPCI</i>
1	if	S		S	then		VS
2	if	S		M	then		S
3	if	S		L	then		M
4	if	M		S	then		S
5	if	M		M	then		M
6	if	M		L	then		L
7	if	L		S	then		M
8	if	L		M	then		L
9	if	L		L	then		VL

Tab. 7: List of degrees of S/N ratio in the fuzzy-based Taguchi method.

### 3.5.1 Input function of stress

As listed in Tab. 2, the maximum, minimum and mean values of S/N ratio of stress are  $-61.67$ ,  $-64.95$  and  $-63.31$  respectively, which are also used to determine the boundaries of the membership degrees, S, M, and L. Then the membership functions of stress are used as the inputs for MPCl. Fig. 9 shows the membership function of stress S/N ratio.

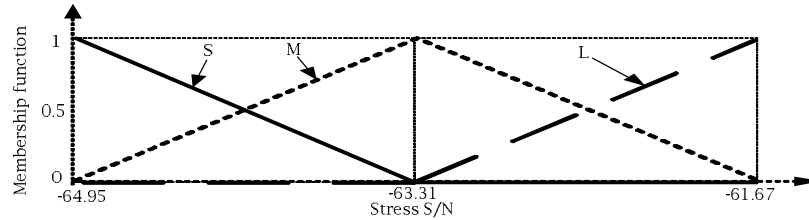


Fig. 9: Membership function of S/N ratio of maximum stress.

### 3.5.2 Input function of reaction force

As shown in Tab. 6., the maximum, minimum and mean values of S/N ratio of reaction force are  $35.00$ ,  $8.21$  and  $21.61$  respectively, which are also used to determine the boundaries of the membership degrees, S, M, and L. Then the membership functions of reaction force are used as the inputs for MPCl. Fig. 10. shows the membership function of S/N ratio of reaction force.

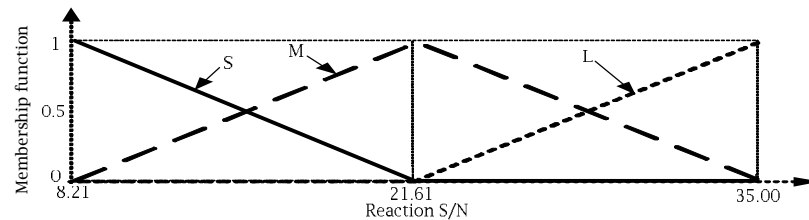


Fig. 10: Membership function of S/N ratio of reaction force.

### 3.5.3 Analysis of outputs

The outputs of the MPCl are classified into 5 degrees: VS, S, M, L and VL. The estimated value among the 5 degrees varies from 0 to 1, as shown in Fig. 11.

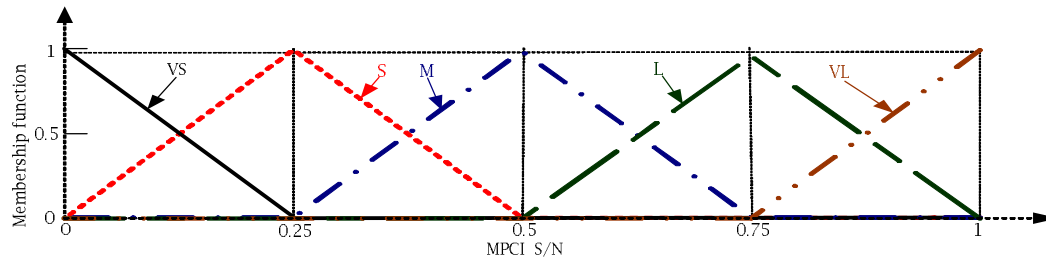


Fig. 11: Membership function of MPCl.

### 3.5.4 Application of fuzzy theory

This research applies the fuzzy theory proposed by Mamdani to integrate two or more quality characteristics into one single. Firstly, the S/N ratio of stress substitutes for Eqs. (4), (5) and (6), to calculate its membership value. The same procedure is applied to Eqs. (7), (8) and (9) with the S/N ratio of reaction force. The membership of MPCl now can be obtained based on the fuzzy rules in Tab. 7. For example, in experiment #1, the S/N ratio of stress is  $-64.09$  (Tab. 2.), thus,  $\mu_{stress\_S} = 0.476$ ; the S/N ratio of reaction force is  $13.47$  (Tab. 6.), hence,  $\mu_{reaction\_S} = 0.607$ . As Tab. 7 suggests, rule #1 states that, if the S/N ratio of stress is small, and the S/N ratio of reaction force is small, the S/N ratio of MPCl should also be small (a common rule is that if the AND operator of Boolean logic exist in fuzzy

logic, membership value of the output is attributable to small membership value of the inputs). Therefore, in this case, the membership value can be obtained as  $\mu_{MPCI\_VS} = 0.476$ .

Similarly, the S/N ratio of maximum stress, -64.09, then,  $\mu_{stress\_M} = 0.524$  and  $\mu_{stress\_L} = 0$  respectively; the S/N ratio of target reaction force, 13.47, then,  $\mu_{reaction\_M} = 0.393$  and  $\mu_{reaction\_L} = 0$  respectively. Finally, according to the fuzzy rules in Tab. 7., the MPCSI membership values can be obtained and illustrated in both Tab. 8 and Fig. 12.

Rule number	Membership value of S/N of max. stress	Membership value of S/N of target reaction force	Membership value of MPCSI
1	if $\mu_{stress\_S} = 0.476$	and $\mu_{reaction\_S} = 0.607$	then $\mu_{MPCI\_VS} = 0.476$
2	if $\mu_{stress\_S} = 0.476$	and $\mu_{reaction\_M} = 0.393$	then $\mu_{MPCI\_S} = 0.393$
3	if $\mu_{stress\_S} = 0.476$	and $\mu_{reaction\_L} = 0$	then $\mu_{MPCI\_M} = 0$
4	if $\mu_{stress\_M} = 0.524$	and $\mu_{reaction\_S} = 0.607$	then $\mu_{MPCI\_S} = 0.524$
5	if $\mu_{stress\_M} = 0.524$	and $\mu_{reaction\_M} = 0.393$	then $\mu_{MPCI\_M} = 0.393$
6	if $\mu_{stress\_M} = 0.524$	and $\mu_{reaction\_L} = 0$	then $\mu_{MPCI\_L} = 0$
7	if $\mu_{stress\_L} = 0$	and $\mu_{reaction\_S} = 0.607$	then $\mu_{MPCI\_M} = 0$
8	if $\mu_{stress\_L} = 0$	and $\mu_{reaction\_M} = 0.393$	then $\mu_{MPCI\_L} = 0$
9	if $\mu_{stress\_L} = 0$	and $\mu_{reaction\_L} = 0$	then $\mu_{MPCI\_VL} = 0$

Tab. 8: Values of MPCSI membership functions.

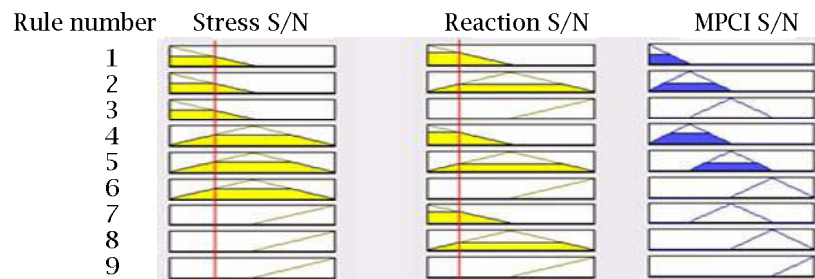


Fig. 12: Results of fuzzy inference.

### 3.5.5 Anti-fuzzy analysis

The last step of fuzzy theory is to reverse the fuzzy inference. The approach applied in this research is to produce a union of areas corresponding to the MPCSI membership values, then to divide the union area into sub-areas, and finally to apply the following formulae to calculate the centroid of the entire area as the S/N ratio of MPCSI:

$$\text{S/N ratio of MPCSI} = \frac{\sum_{i=1}^n A_i \bar{x}_i}{\sum_{i=1}^n A_i} \quad (3)$$

where  $A_i$  = sub-areas after area unionizing, and  $\bar{x}$  = centroid of each sub-area in x direction.

Taking experiment #1 as an example, according to Fig. 12, rules #1, #2, #4 and #5 can create areas for unionizing. Then the union area is divided into 3 sub-areas, a triangle, a trapezium and a parallelogram, displayed in Fig. 13. Eq. (3) is next used to find the S/N ratio=0.33.

The same procedure is applied to generate the S/N ratio of MPCSI for each S/N ratio of stress and reaction force, and the results are summarized in Tab. 9.

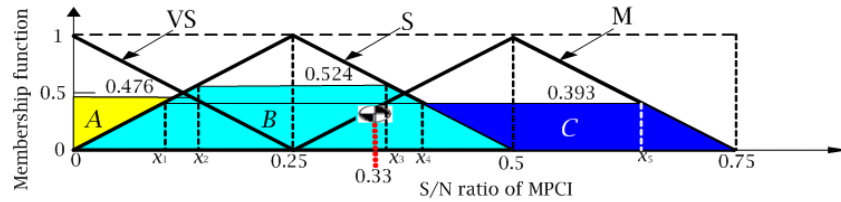


Fig. 13: Sub-areas and their centroids.

Exp.	S/N ratio of max stress	S/N ratio of reaction force	S/N ratio of MPCI	Exp.	S/N ratio of max stress	S/N ratio of reaction force	S/N ratio of MPCI
1	- 64.01	13.03	0.330	10	- 63.86	16.34	0.354
2	- 63.64	15.08	0.375	11	- 64.62	21.42	0.341
3	- 62.97	12.82	0.376	12	- 63.26	10.68	0.382
4	- 64.38	25.88	0.49	13	- 64.42	51.21	0.508
5	- 62.48	9.43	0.399	14	- 61.59	8.15	0.49
6	- 64.48	15.93	0.360	15	- 64.66	20.60	0.306
7	- 63.19	11.98	0.335	16	- 61.53	8.08	0.500
8	- 64.75	26.56	0.573	17	- 64.50	26.76	0.509
9	- 63.25	11.22	0.322	18	- 64.73	25.26	0.415

Tab. 9: List of MPCI results.

3.5.6 Optimal design results

The S/N ratios of MPCI in Tab. 9 can be used to calculate the values in the response table and S/N response graph of each control factor at each level. Tab. 10 lists the calculated S/N ratios of MPCI of 8 control factors at different levels. And Fig. 14 is a response graph of those S/N ratios. From the figure, the optimal combination of spring dimensions is A2 B3 C2 D3 E2 F1 G3 H3. Then the finite element analysis is applied to calculate its maximum stress as 1,600.4MPa, and its maximum reaction force as 0.6628N (67.57gf). The results show that the reaction force is highly close to the target value 70gf, and the maximum stress is reduced accordingly. In other words, the fuzzy-based Taguchi method can sufficiently manage the multi-objective about stress and reaction force, and its results advance the analysis by simplex Taguchi methods.

Control Factor	A	B	C	D	E	F	G	H
Level 1	0.40	0.36	0.42	0.38	0.38	0.44	0.40	0.40
Level 2	0.42	0.43	0.45	0.40	0.44	0.41	0.37	0.40
Level 3		0.44	0.36	0.44	0.41	0.38	0.45	0.43

Tab. 10: S/N ratio of MPCI of 8 control factors at various levels.

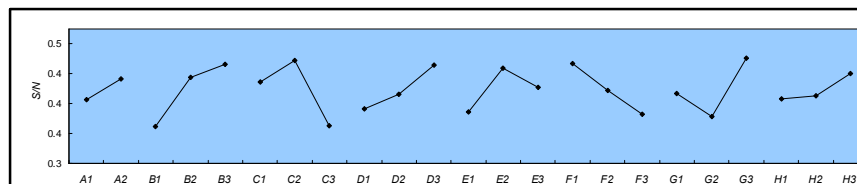


Fig. 14: Response graph of S/N ratio of MPCI.

#### 4 CONCLUSIONS

This research targets the driven source of slide-cover cell phones, the driving spring, to optimize its design. Firstly, aiming for minimization of reaction force, a simplex Taguchi method is applied to obtain the optimal combination of the spring dimensions as A1 B2 C1 D3 E2 F2 G1 H3, the spring of which generates a maximum stress 1,150.1MPa and maximum reaction force 33.21gf. Although the stress is reduced significantly, the reaction force is too small to move the slider. Then, to reach adequate reaction force, a similar procedure is employed to obtain yet another combination of the spring dimensions as A2 B3 C2 D1 E1 F1 G3 H1, the spring of which produces a maximum stress 1,840.3MPa and maximum reaction force 71.5gf. Even though the reaction force achieves its target value, the maximum is extremely high which may cause damage to the spring. In order to solve the conflict of above dilemmas, this research introduces the “fuzzy-based Taguchi method” to optimize the design for the driving spring, the approach with which both requirements for stress and reaction force can be fulfilled. Based on this methodology, the optimal combination of the spring dimensions is A2 B3 C2 D3 E2 F1 G3 H3, the spring of which creates maximum stress 1,600.4MPa and maximum reaction force 67.57gf. As a result, the reaction force is extremely close to the target value, 70gf, while the stress is relatively small. In conclusion, the results prove that the fuzzy-based Taguchi method is a sufficient approach to manage the inter-relationship between stress and reaction force of the driving spring, and to achieve the objective of design optimization.

#### REFERENCES

- [1] Cook, R.D.: Finite Element Modeling for Stress Analysis, John Wiley & Sons, Inc., New York, 1995.
- [2] Mac Donald, B.J.: Practical Stress Analysis with Finite Elements, Glashevin Publishing, Dublin, Ireland, 2007.
- [3] Wah, B.W. (ed.): Wiley Encyclopedia of Computer Science and Engineering, John Wiley and Sons, New York, 2009, 1253-1264.
- [4] Ou, H.; Balendra, R.: Perform Design for forging of aerofoil sections using Finite Element simulation, Journal of Materials Processing Technology, 80-81, 1998, 144-148.
- [5] Hsu, Y.L.; Hsu, Y.C.; Hsu, M.S.: Shape Optimal Design of Contact Springs of Electronic Connectors, Journal of Electronic Packaging, 124, 2002, 178-183. DOI:10.1115/1.1463730
- [6] Ross, P.J.: Taguchi Techniques for Quality Engineering, McGraw-Hill, Inc., New York, 1996.
- [7] Lin, J.L.; Wang, K.S.; Yan, B.H.; Tarn, Y.S.: Optimization of the Electrical Discharge Machining Process Base on the Taguchi Method with Fuzzy Logics, Journal of Materials Processing Technology, 102(1-3), 2000, 48-55. DOI:10.1016/S0924-0136(00)00438-6
- [8] Kunjur, A.; Krishnamurty, S.: A Robust Multi-Criteria Optimization Approach, Mechanism and Machine Theory, 32(7), 1997, 797-810. DOI:10.1016/S0094-114X(97)00007-4
- [9] Tarn, Y.S.; Yang, W.H.; Juang, S.C.: The Use of Fuzzy Logic in the Taguchi Method for the Optimization of the Submerged Arc Welding Process, International Journal of Advanced Manufacturing Technology, 16, 2000, 688-694. DOI:10.1007/s001700070040
- [10] Derringer, G.; Suich, R.: Simultaneous Optimization of Several Response Variables, Journal of Quality Technology, 12, 1980, 214-219. DOI:10.2307/1268392
- [11] Elsayed, E.A.; Chen, A.: Optimal Levels of Process Parameters for Products with Multiple Characteristics, International Journal of Production Research, 31, 1993, 1117-1132. DOI:10.1080/00207549308956778
- [12] Khuri, A.I.; Conlon, M.: Simultaneous Optimization of Multiple Response Represented by Polynomial Regression Functions, Technometrics, 23(4), 1981, 363-375. DOI:10.2307/1268226
- [13] Tong, L.L.; Su, C.T.; Wang, C.H.: The Optimization of Multi-Response Problems in the Taguchi Method, International Journal of Quality and Reliability Management, 14, 1997, 367-380.
- [14] Kao, J.Y.; Pan, Y.D.: Optimization of Tool Geometry in Face Milling Operation Using the Fuzzy-Based Taguchi Method, Journal of Technology, 16, 2001, 709-716.